

## Performance evaluation of pedestrian bridge as vertical evacuation site during the 2011 tsunami in Japan

Abdul MUHARI\*  
Shunichi KOSHIMURA\*  
Fumihiko IMAMURA\*

\*Graduate School of Engineering, TOHOKU University

(Received March 31, 2012 Accepted July 20, 2012)

### ABSTRACT

We evaluated the performance of pedestrian bridges as vertical evacuation sites during the 2011 Tohoku tsunami in six prefectures in Japan. Evaluation was performed by considering the vulnerability and tsunami hazard characteristics as parameters that influence the damage probability. Vulnerability is represented by the exposure, indicated by the bridge's position from the shoreline relative to the maximum inundation distance. In contrast, tsunami hazard was identified from the observed flow depths relative to the bridge's height. We found that pedestrian bridges that were positioned inside an area less than 0.2 times that of the maximum inundation distance (which is 6 km), or where the tsunami flow depth exceeded that of the bridge's height by more than 1.5 times, have a high probability of being damaged by a tsunami. It is necessary to consider such limitations when determining the placement criteria of pedestrian bridges as evacuation shelters for the above areas. Starting with the concept of sudden expansion phenomenon, a series of numerical exercises was conducted to parameterize hydraulic conditions that affect the sudden drop in water level due to the building configuration at an intersection. We searched the areas where pedestrian bridges could still be used for evacuation with the existing height. Preliminary results indicate that if the sudden expansion ratio ( $D$ )  $> 1.5$ , and the ratio between the widths of road to the width of residential blocks ( $\beta$ )  $< 0.1$ , sudden expansion occurs with hydraulic gradient dependent on the Froude number ( $Fr$ ). In this condition, the bridges can be used for evacuation as long as they are installed on the side of the road parallel to the coastline, or on the landward side of the road at an intersection. These results provide the opportunity to apply more distributed evacuation shelters to relatively flat and populated areas.

**Keywords:** tsunami evacuation, pedestrian bridge, fragility curve, sudden expansion

### 1. Introduction

Geographical aspects and level of awareness in responding to a tsunami warning are influential parameters in determining the successful rate of evacuation. In the central to northern part of the Sanriku

coast in Iwate Prefecture, the villages are surrounded by hills. Hence, they are easily reached once a tsunami evacuation order has been issued. However, in the southern part of the Sanriku coast, and especially on the Sendai plain, Miyagi Prefecture, high ground is situated far from the coast and the designated verti-

cal evacuation sites are not well distributed. During the 2011 tsunami, therefore, people in the plain areas tended to use cars to evacuate. While cars are very important for evacuating elderly people who cannot walk long distances, they can cause problems such as traffic jams that will delay the evacuation to safety. A joint survey conducted by the Cabinet Office, Internal Affairs and Communication Ministry, Fire and Disaster Management Agency and Meteorological Agency in July 2011 revealed that among the 870 respondents, 55.7% of them evacuated by car and 34% were stuck in traffic jams (Cabinet Office, 2011). Most people who used cars said that they returned home to look for family members and collect them. A similar tendency of people using cars to evacuate was also revealed in Kesenuma City; a survey conducted by the municipal government and Ministry of Land, Infrastructures and Transport indicated that 45% of 6,730 survivors who evacuated by car – apart from the 6% who abandoned their cars and evacuated on foot – stated that cars were necessary to evacuate elderly people and children because evacuation sites were far away (MLIT, 2011). The above experiences could be interpreted in two linked ways: first, it is impossible to avoid the use of cars during evacuation due to physical and psychological reasons. Second, the more cars involved during evacuation, the greater the possibility of traffic jams. Therefore, in order to ensure the safety of evacuees in plain areas, it is necessary to develop more distributed temporary evacuation sites.

Along the national and prefectural roads in Japan, pedestrian bridges have been installed at an average height of 4.5 to 5 m. Depending on the local height of tsunami inundation; pedestrian bridges

can be utilized as temporary vertical evacuation sites. Figure 1 shows a snapshot of an amateur video taken from a pedestrian bridge in Yuriage, Miyagi Prefecture, during the 2011 Tohoku tsunami in Japan.

During the evacuation, most traffic jams occurred at intersections (Southworth, 1991). Where pedestrian bridges are available at intersections inside tsunami affected areas, the evacuees can simply leave their cars and climb-up onto the bridge if they become trapped at an intersection due to a traffic jam. We assumed that pedestrian bridges were an appropriate solution for rapid evacuation in plain areas, especially when it is difficult to prohibit the use of cars. To verify our hypothesis, we conducted a study to evaluate the performance of pedestrian bridges during the 2011 tsunami in six prefectures in Japan, namely Ibaraki, Fukushima, Miyagi, Iwate, Aomori and Hokkaido. Fifty-two bridges including those in train stations were examined by considering the vulnerability indicated by the exposure (position from the shoreline), and the hazard in terms of tsunami flow depths around the bridge as parameters that influence the damage probability.

Previous studies have assessed the structural fragility in particular buildings subjected to tsunami flow (e.g., Shuto, 1993, Koshimura et al. 2009). In the context of bridge structures, their fragility to seismic ground motion and Peak Ground Acceleration (PGA) parameters were also well assessed (e.g., Shinozuka et al. 2000, Karim and Yamazaki. 2003). In the context of bridge fragility subjected to tsunami force, Shoji and Moriyama (2007) analyzed bridge performance during the 2004 Indian Ocean tsunami in Banda Aceh and Sri Lanka. In their study, tsunami force is



**Figure1.** Tsunami wave front observed from survivor in pedestrian bridge at Yuriage town, Miyagi.

(source. <http://www.youtube.com/watch?v=DXbeoKgQ9x0>)

represented by the estimated flow depth obtained by adjusting the field survey data to the still water level of the river where bridges were installed. In another study, based on field observation of damage to bridges in Banda Aceh after the 2004 Indian Ocean tsunami, Iemura and Pradono (2005) reported that prevention of the seismic unseating problem might be applicable to tsunami force as well. Under the Development of Performance Based Tsunami Engineering (PBTE, NEES, 2010), a set of hydraulic experiments in addition to numerical models were conducted to obtain in-depth analysis of fluid-structural interaction with the focus on the tsunami effect on coastal infrastructures (dry bed). Since tsunami generated impact on structures may differ in wet- and dry-beds, the estimation of tsunami impact on structures in dry beds is still under development.

In our study, the performance of a bridge on a dry bed subjected to a tsunami was evaluated quantitatively. We limited our interest to the performance of a pedestrian bridge struck by a tsunami based on field observation data supported by remote sensing analyses, and determined conditions that influence the damage probability of pedestrian bridges. Then, we conducted a set of numerical exercises to optimize their function by studying the tsunami flow characteristics at intersections where the bridges are situated. The findings were then used as a basis to determine placement criteria should such structures be selected for use as temporary evacuation shelters.

## 2. Data and methodology

### 2.1. Data

We first compiled 68 pedestrian bridges assumed to be constructed inside tsunami affected areas based on satellite image analysis and field survey data. The searching process was supported by the street view

facility available on Google maps (Google, 2012). The database included 21 pedestrian bridges at train stations from 6 prefectures as listed in Table 1. Next, we conducted a cross-check analysis to ensure the bridges were placed inside the inundation zone by superimposing them with the results of a post-tsunami survey conducted by the Japan Society of Civil Engineers (JSCE, 2011). If placement was affirmed, we then confirmed whether there were field observation points available around the bridge.

As a result, 16 bridges were excluded from further analysis since there was insufficient run-up or flow depth data on them. For those that were selected for the subsequent steps, we interpolated the closest run-up or flow depth observation points near the pedestrian bridges using a simple interpolation scheme shown by Eq.1,

$$h = [\sum_i^n r_i] / n \quad (1)$$

Here,  $h$  is the actual flow depth around the bridge,  $n$  is the number of observed run-up or flow depth data and  $r$  is the observed values of run-up height and flow depths. The results of cross-check analysis and calculated observed flow depths are given in Table 2.

In terms of exposure, we measured the distance of bridges from the shoreline by generalizing the beach strike to the north without considering specific features such as small rivers, ports, ponds and so forth.

### 2.2. Methodology

#### 2.2.1. Developing fragility curves for pedestrian bridges

After compiling the field observation data in addition to the satellite image analysis and oblique photographs provided by the Geographic Survey Institute of Japan (GSI, 2011), damage levels of pedestrian

**Table 1** Number of collected bridges along the east coast of Japan

No	Prefecture	Pedestrian bridge (at intersection)	Pedestrian bridge (at train station)	Total
1	Hokkaido	4	0	4
2	Aomori	0	1	1
3	Iwate	11	2	13
4	Miyagi	22	8	30
5	Fukushima	10	2	12
6	Ibaraki	0	8	8
<b>Total</b>				<b>68</b>

**Table2.** Observed bridges and flow depth during 2011 tsunami

No	City / town	Longitude	Latitude	Flow depth (m)	Distance from shoreline (m)	Damage level
1	Oyakaigan	141.5672	38.8138	11.32	25	B
2	Miyako	141.9628	39.6406	3.50	47	C
3	Miyako	141.9604	39.6377	3.40	137	C
4	Miyako	141.9570	39.6422	4.30	146	C
5	Hachinohe	141.5554	40.5305	4.68	149	C
6	Rikuzentakata	141.6488	39.0087	14.39	230	A
7	Rikuzentakata	141.6500	39.0090	14.39	240	A
8	Ofunato	141.7205	39.0566	6.90	304	C
9	Kitaibaraki	140.7483	36.7898	5.87	304	C
10	Fukushima	140.9846	37.1009	3.35	327	C
11	Yamada	141.9506	39.4641	5.71	396	A
12	Fukushima	140.9964	37.1437	5.27	433	C
13	Fukushima	140.9957	37.1427	5.27	448	C
14	Osuchi	141.9025	39.3567	7.80	484	A
15	Shinshi	140.9266	37.8812	8.50	554	B
16	Minamikesenuma	141.5767	38.8950	5.80	619	A
17	Takahagi	140.7191	36.7179	2.85	662	C
18	Ishinomaki	141.3655	38.4180	1.84	671	C
19	Kitaibaraki	140.7791	36.8322	3.75	676	C
20	Sakamoto	140.9126	37.9283	4.17	720	B
21	Otsuchi	141.9001	39.3577	7.84	732	A
22	Ishinomaki	141.3351	38.4194	4.10	750	B
23	Ishinomaki	141.3332	38.4196	4.10	769	B
24	Fukushima	140.8960	36.9506	2.88	820	C
25	Sendai	141.0349	38.2990	1.83	871	C
26	Kesenuma	141.5821	38.9192	2.94	998	B
27	Fukushima	140.7897	36.8980	2.90	1004	C
28	Ishinomaki	141.3217	38.4213	1.32	1042	C
29	Sendai	141.0325	38.2926	2.13	1100	C
30	Sendai	141.0056	38.2841	1.40	1172	B
31	Fukushima	140.7925	36.9029	2.90	1175	C
32	Ishinomaki	141.2666	38.4305	1.04	1226	C
33	Yamashita	140.9008	37.9672	3.51	1263	C
34	Sendai	141.0037	38.2855	1.14	1301	C
35	Kamaishi	141.8717	39.2734	5.07	1301	C
36	Ishinomaki	141.2736	38.4302	2.80	1302	B
37	Soma	140.9480	37.8228	4.75	1405	C
38	Sendai	141.0200	38.3097	1.08	1483	C
39	Sendai	140.9832	38.2793	3.75	1523	C
40	Sendai	141.0154	38.2925	3.11	1603	C
41	Ishinomaki	141.3158	38.4267	2.50	1680	C
42	Natori	140.9437	38.1792	2.22	1750	B
43	Ishinomaki	141.3133	38.4301	3.90	2053	C
44	Sendai	141.0090	38.2898	2.41	2091	C
45	Kesenuma	141.5679	38.8936	1.53	2191	C
46	Hamayoshida	140.8902	38.0020	1.57	2212	C
47	Ishinomaki	141.3046	38.4353	1.72	2323	C
48	Hmatsushima	141.2140	38.4210	1.33	2584	C
49	Hmatsushima	141.2079	38.4187	0.78	2610	C
50	Hmatsushima	141.2195	38.4229	2.80	2650	C
51	Kesenuma	141.5640	38.9003	0.72	2846	C
52	Fukushima	140.9715	37.7014	4.90	3456	C

**Table3.** Damage criteria of pedestrian bridge

No	Damage Classification	Indicator
1	Heavily damage (swept away)	A
2	Slight damage (i.e., stairs)	B
3	Survived (only inundated)	C

bridges were classified into three types (see Table3): (A) is heavy damage, which describes the condition where bridges are swept away or their decks are damaged, (B) is partial damage indicated by damage to the stairs or barriers so repair is required before re-use, and (C) is the condition where bridges are inundated only and can be directly used after a tsunami.

We first analyzed the fragility of pedestrian bridges in terms of tsunami hazard. In general, a higher tsunami flow depth will increase the damage probability of a pedestrian bridge. In other words, damage probability should have a linear correlation with the increment of tsunami flow depth. Even though the damage itself might be caused by the impact of debris collision, in this study we used tsunami flow depth as the only observable parameter from the field survey. Some of the debris trapped on the bridge's stairs was visible from satellite imagery, but incomplete figures for all of them might yield inconsistent interpretation. Therefore, debris impact is excluded from the analysis. The cumulative damage probability is given through the widely used fragility equation as follows,

$$P_i(x) = \Phi \left[ \frac{\ln x - u'}{\sigma'} \right] \quad (2)$$

Here,  $P$  is the cumulative probability of specific damage classification ( $i$ ),  $\Phi$  is the standardized lognormal distribution function,  $x$  is the median of the observed tsunami flow depth,  $u'$  and  $\sigma'$  are the median and standard deviation of random variable of  $x$ , respectively. In order to obtain the last two statistical parameters, we first calculated the inclination ( $u_y$ ) and intercept ( $\sigma_y$ ) through the least-square fitting plot of  $\ln x$  and the inverse of lognormal distribution function  $\Phi^{-1}$ . Next the median and standard deviation were determined by ( $^{-u_y/\sigma_y}$ ) and ( $^{1/\sigma_y}$ ), respectively (e.g., Shoji and Moriyama, 2007).

For pedestrian bridge fragility in terms of exposure, the previously mentioned approaches should be modified since the damage probability will be reduced together with the increment of the distance from the shoreline. In other words, the safety probability will increase if bridges are placed farther from the coast. Equation 2 therefore is modified as follows,

$$1-[P_i(x)] = 1- \Phi \left[ \frac{\ln x - u'}{\sigma'} \right] \quad (3)$$

By applying these equations, fragility curves for pedestrian bridges are developed and discussed in the following chapters.

### 2.2.2. Searching criteria of pedestrian bridge for tsunami evacuation

In order to ensure the safety of evacuees when using pedestrian bridges as evacuation sites, the deck's height should be higher than the maximum surrounding tsunami flow depth. However, in Japan the height of pedestrian bridges is almost the same in the range of 4.5 – 5 m. In this case, there are two options available if pedestrian bridges are to serve as evacuation shelters. First is adjusting the height according to the maximum estimated tsunami flow depth. This option implies that the bridge height might be increased and become unsuitable for the elderly. The second option is searching for an appropriate location where the maximum tsunami flow depth is lower than the bridge's height. However, this requires further placement criteria to utilize the bridge at the existing height. This section focuses on the second option, which will be further elaborated.

In populated areas where streets between two residential blocks are fenced by rows of houses, tsunamis might have specific features when they pass through narrow roads. For instance, flow depth along a road prior to an intersection might be higher than the flow depth after the intersection. Here, a sudden expansion might occur because of the spread of water mass in different directions and the building configuration around the intersection (e.g., Muhari et al. 2011). Therefore, we assumed that once the influential factors affecting the flow characteristics at an intersection can be parameterized, the placement criteria of pedestrian bridges can be established.

Many engineering applications have shown that sudden expansion generally depends on the expansion ratio, which is described as the ratio between channel width before and after expansion. However, most of the previous researches conducted experiments using a closed tube to keep the flux constant before and after the expansion (e.g., Oliveira and Pinho, 1997). Thus, the head loss was only determined by the expansion ratio. In the tsunami case, however, more complex aspects need to be considered i.e., housing geometry at an intersection, effect of the width of residential blocks, and so forth. Goto and Shuto (1983)

conducted both a hydraulic experiment and numerical analysis to parameterize factors that influence the expansion coefficient when a tsunami flows along lined obstacles. However, their works were limited to two parallel obstacles where there was no actual representation of an intersection after the rearmost region.

In this study, we performed numerical exercises to preliminarily parameterize the influential factors on tsunami characteristics at an intersection. A hypothetical town was set up as shown in Fig 2. Residential blocks prior to the intersection occupied all areas, while the one after the intersection is not. This design allows the flux at an intersection to spread out in different directions, and minimize the unnecessary reflecting flows from the side walls. In reality, this design is only able to represent areas where the width of the residential block is much larger than the width of the road between them.

A set of non-linear shallow water equations as given by Imamura (1996) was used to model the propagation and inundation of the tsunami. The tsunami is initialized by a sine wave as shown in Fig. 2.

The reliability of 2D Shallow Water Equation (SWE) to represent flow passing through obstacles had been demonstrated by Goto and Shuto (1983), and Tsudaka et al. (2011). They validated the result of numerical calculation using SWE with experimental data and obtained good agreement. However, his approach has limitations on reproducing flood water behind buildings (Tsudaka et al. 2011). Also, the absence of the momentum diffusion term in the SWE might yield a less accurate modeled water level due to the lack of lateral diffusion at intersections.

The numerical simulations were conducted in several scenarios, and the initial tsunami wave was propagated at various amplitudes as given in Table 4.

The influence of the expansion ratio ( $D$ ) was assessed by increasing the road width after the intersection ( $d_2$ ); while the road width prior to the intersection ( $d_1$ ) remained unchanged. The effect of roads parallel to the coast ( $l_2$ ) was analyzed by increasing their width while the length of residential blocks prior to the intersection ( $l_1$ ) was constant. We also investigated the effect of the reduction of the length of a residen-

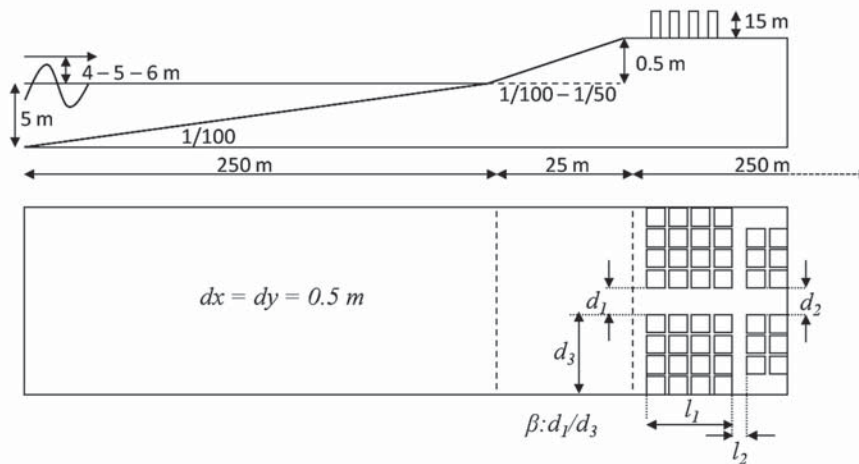


Figure 2. Design of hypothetical town for numerical simulation of tsunami at intersection

Table 4. Scenarios for numerical simulation of tsunami at intersection

Case	Slope 0					Slope 1/50		Slope 1/100	
	$d_2/d_1$ (D)	$l_1/l_2$	$l_2/l_1$	$\beta$	Amplitude (A) (meter)	$d_2/d_1$ (D)	Amplitude (A) (meter)	$d_2/d_1$ (D)	Amplitude (A) (meter)
Case 1	1.20	5.9	0.17	0.11	2, 3, 4, 5, 6	1.20	5.00	1.20	5.00
Case 2	1.40	4.7	0.22	0.16	2, 3, 4, 5, 6	1.40	5.00	1.40	5.00
Case 3	1.60	3.5	0.27	0.21	2, 3, 4, 5, 6	1.60	5.00	1.60	5.00
Case 4	1.80	2.3	0.32	0.24	2, 3, 4, 5, 6	1.80	5.00	1.80	5.00
Case 5	2.00	-	-	0.28	2, 3, 4, 5, 6	2.00	5.00	2.00	5.00
Case 6	2.20	-	-	-	2, 3, 4, 5, 6	2.20	5.00	2.20	5.00

tial block on the head-loss at an intersection if parts of them were damaged by a tsunami. Lastly, we estimated the effect of the ratio between road widths ( $d_1$ ) to the width of residential blocks ( $d_3$ ) symbolized by ( $\beta$ ) on influencing the hydraulic gradient at a specific expansion ratio ( $D$ ). From the results of the modeled water surface of each scenario, a cross section at the middle of the road perpendicular to the shoreline was extracted for analysis. The numerical scenarios were applied to flat and sloping (1/100 and 1/50) topography with a cell size of 0.5 m. Grid size was selected according to an empirical relation of  $dx/(g h_{max})^{1/2} T < 3 \times 10^{-3}$  to obtain  $0.5 < \text{predicted value/measured value} < 2$  as proposed by Fujima (2012). The wave period of 0.5 hours was selected for the sin wave initially. This period is similar to the average observed period of the first wave during the 2011 Tohoku tsunami at Sendai buoys.

**3. Results and discussions**

**3.1. Fragility curves**

We classified the damage rank, cumulative frequency and cumulative damage probability in a 1 meter range as shown in Table 5. In terms of their location, damage rank, cumulative frequency and cumulative damage probability were analyzed at intervals of 250 m (Table 6).

Regression analysis gives the parameters shown in Table 7 which were used to determine the best fit of the fragility curve with the obtained coefficient correlations (R2) for the exposure component as 0.74 and 0.61 for damage classification (A) and cumulative (A+B). In terms of susceptibility, the coefficient correlations were obtained as 0.64 for damage classification (A) and 0.81 for cumulative damage classification (A+B).

The fragility curves were then developed by plotting the damage probability to the non-dimensional number for each fragility parameter. The non-dimensional number for exposure is defined as the ratio between the locations of the respective bridge from the shore ( $l$ ) to the maximum tsunami inundation distance ( $L$ ), which is assumed to be 6 km. As for the fragility curve subjected to tsunami hazard, the non-dimensional parameter is given by the ratio between the observed tsunami run-ups ( $h$ ) to the height of the pedestrian bridge ( $H$ ). The results are shown in Fig. 3 as follows,

The above results reveal that most pedestrian bridges have a more than 50% probability of being damaged by a tsunami if they were placed closed to the shore. This is a common understanding on vulnerability analysis. However, an important point to note is up to what distance the risk of using a pedestrian bridge for evacuation is relatively high. Here, our

**Table5.** Number of analyzed bridges and their cumulative damage probability subjected in term of tsunami hazard characteristic

Observed inundation depths (m)	Frequency (number of bridges)			Cumulative frequency			Cumulative damage probability		
	(A)	(B)	(C)	A	A+B	A+B+C	A	A+B	A+B+C
	Heavily damage	Slight damage	Survived only inund.						
0-1	0	0	2	0	0	2	-	-	1
1-2	0	1	10	0	1	11	-	0.09	1
2-3	0	3	8	0	3	11	-	0.27	1
3-4	0	0	8	0	0	8	-	-	1
4-5	0	3	4	0	3	7	-	0.43	1
5-6	1	1	4	1	2	6	0.17	0.33	1
6-7	0	0	1	0	0	1	-	-	1
7-8	2	0	0	2	2	2	0.99	1.00	1
8-9	0	1	0	0	1	1	-	1.00	1
9-10	0	0	0	0	0	0	-	-	-
10-11	0	0	0	0	0	0	-	-	-
11-12	0	1	0	0	1	1	-	1.00	1
12-13	0	0	0	0	0	0	-	-	-
13-14	0	0	0	0	0	0	-	-	-
14-15	2	0	0	2	2	2	0.99	1.00	1
Total	5	10	37	5	16	52	-	-	-

**Table6.** Number of analyzed bridges and their cumulative damage probability in term of exposure

Distance from the shoreline (m)	Frequency (number of bridges)			Cumulative frequency			Cumulative damage probability		
	(A) Heavily damage	(B) Slight damage	(C) Survived only inund.	A	A+B	A+B+C	A	A+B	A+B+C
0-250	2	1	4	2	3	7	0.29	0.43	1
250-500	3	1	4	3	4	8	0.38	0.50	1
500-750	1	3	3	1	4	7	0.14	0.57	1
750-1000	0	2	2	0	2	4	-	0.50	1
1000-1250	0	0	5	0	0	5	-	-	1
1250-1500	0	1	5	0	1	6	-	0.17	1
1500-1750	0	1	4	0	1	5	-	0.20	1
1750-2000	0	0	0	0	0	0	-	-	-
2000-2250	0	0	4	0	0	4	-	-	1
2250-2500	0	0	1	0	0	1	-	-	1
2500-2750	0	0	3	0	0	3	-	-	1
2750-3000	0	0	1	0	0	1	-	-	1
3000-3250	0	0	0	0	0	0	-	-	-
3250-3500	0	0	1	0	0	1	-	-	1
Total	6	9	37	6	15	52	-	-	-

**Table7.** Statistical parameters for fragility function obtained from regression analysis

Variable of fragility (x)	$\mu^r$	$\sigma^r$	$R^2$
Exposure (distance from the shoreline)			
- Damage classification (A)	4.12	1.53	0.74
- Cumulative (A) + (B)	5.24	1.13	0.61
Hazard (tsunami inundation)			
- Damage classification (A)	1.72	0.33	0.64
- Cumulative (A) + (B)	1.20	0.42	0.81

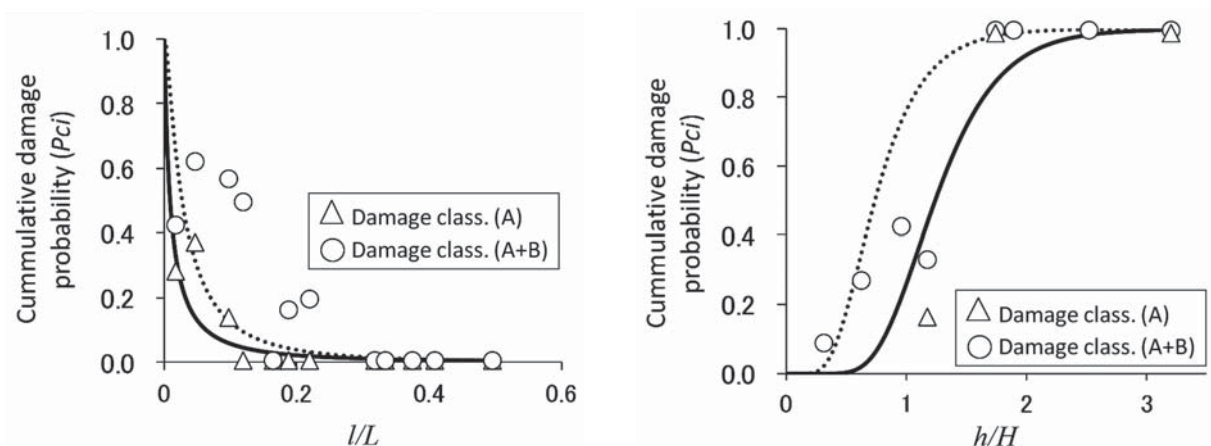


**Figure3.** Fragility curves for exposure (left) and susceptibility (right) parameters. Solid line indicates the fragility for criteria (A) and dashed line for cumulative (A) + (B)

result shows that up to 1.2 km from the shore (or 0.2 times that of the assumed maximum inundation extent); the probability of a pedestrian bridge being damaged by a tsunami remains high. The damage probability is more than 50% for those within an area of 0.1 times that of the maximum inundation extent.

Even though the coefficient correlations ( $R^2$ ) for both fragility parameters are relatively good, some data are scattered especially when it represents the cumulative damage (A and B) in the exposure component. The cause for this is attributed to two possibilities: first, the bridges located far from the shore still incurred some damage. Second, bridges that were situated near the coast were not damaged by the tsunami. For the first possibility, we visualized examples of bridges in Ishinomaki City that incurred damage (B) even though they were placed 1 to 1.5 km from the shore. Using satellite images after the disaster, it can be seen that a bridge was hit by a house that was swept along by the tsunami (Fig. 4). For the second possibility, on the contrary, some bridges in Miyako City were much closer to the shore (< 100 m), but no damage was observed. Even though several available amateur videos showed that much floating debris such as fishing boats was brought inland by the tsunami, fortunately none of it directly hit the bridges. Based on the above facts, we should note that the above described quantitative analysis only shows the correlation between some observable parameters from the field observation data or remote sensing analysis to the damage degree of pedestrian bridges. This might not be sufficient to describe the exact factors

that destroy or damage bridges such as debris collision. However, it is still assumed that the selected fragility components can represent such unobservable parameters quantitatively due to the limitation of scientific evidence. This is the reason why we acquired scattered data on the fragility curves. Further detailed analysis especially of the debris source and its impact is required to analyze the mechanism of damage to pedestrian bridges.

The result from the exposure perspective can also be described to some extent by the developed fragility curves for the tsunami hazard component. Here, we learned that for criteria (A), pedestrian bridges have a more than 50% probability of being swept away by a tsunami if the surrounding flow depths are 1.5 times that of the height of the bridge's deck or around 6 to 7.5 m. This height of the tsunami was experienced by almost all areas on the Sanriku coast within a distance of 0.5 to 1 km from the shore (e.g. Mori et al. 2011). If the cumulative damage is taken into account, it can be seen that the bridge will start to have a high probability of being damaged by a tsunami if the observed run-up height is close to the height of the bridge.

The above results have various implications. First, the use of pedestrian bridges in an area close to the shore (up to 1.2 km from the shore), or bridges placed in areas with predicted flow depth close to their height may still be dangerous as vertical evacuation sites. In reality, however, areas within 1 km of the shore—where the 3 to 5 m tsunami run-up is more likely to occur—might be critical for rapid evacuation. Particularly in plain areas, this region might have lim-



**Figure 4.** Debris collision observed from satellite image (left) and oblique photographs (right, GSI) after tsunami in Ishinomaki.

ited evacuation time and potential problems such as traffic jams during evacuation. Therefore, to support the need for pedestrian bridges for evacuation in this area, we determined the placement criteria to apply pedestrian bridges as evacuation sites in the area described above.

### 3.2 Placement criteria for pedestrian bridge

We first analyzed the influence of the expansion ratio ( $D$ ) as given in Fig. 5, panel [1]. If  $d_1$  (symbols refer to Fig. 2) is relatively similar to  $d_2$ , then the hydraulic gradient ( $\text{tg } \alpha$ ) will not be observed (see description of  $\text{tg } \alpha$  in Fig. 5, panel [2]). It will start to be visible if the expansion ratio ( $D$ ) is 1.4, and saturated when  $D$  equals 2. Therefore, in a similar range of Froude number ( $\text{Fr}$ ) examined in this study, a higher expansion ratio ( $D > 2$ ) will not give an even higher hydraulic gradient. These indicate that the influence of the expansion ratio is crucial; if a pedestrian bridge is to be positioned at an intersection with sudden expansion phenomena, then the most appropriate place for the pedestrian bridge is on the landward side and the side parallel to the coastline of an intersection. On these sides, the maximum predicted tsunami flow depths will be lower than that on the sea-side of the intersection.

The subsequent analyses took into account the effect of road width parallel to the coastline ( $l_2$ ), and the effect of road length prior to the intersection ( $l_1$ ) on influencing the hydraulic gradient. Our results show that there was no significant effect from these factors. This means first, the water mass that flows along roads parallel to the coastline will not significantly influence the observed hydraulic gradient at the intersection; it simply creates a slight difference in the initial position of the hydraulic jump, which is not considered in this study (Fig. 5, panel [2]). Second, the road length prior to the intersection ( $l_1$ ) does not influence the hydraulic gradient. Their effect is limited only to a slight reduction of the flow depth depending on the road length (Fig. 5, panel [3]). This was explained by Goto and Shuto (1983). They stated that when a tsunami flows between lined obstacles, the only energy loss is caused by friction due to roughened walls, which is considered to be negligible. Nevertheless, even if some houses along the road prior to the intersection are damaged by a tsunami, the sudden expansion phenomena will still occur as

long as the expansion ratio at the intersection meets the requirements discussed previously.

Considering the influence of Froude number ( $\text{Fr}$ ), we conducted numerical experiments in the range of  $\text{Fr}$  higher than its critical condition ( $> 1$ ). This is because the bore is usually observed under supercritical flow. The correlation between  $\text{tg } \alpha$  and expansion ratio ( $D$ ) in the range of Froude number 1.13 to 1.34 is given in Fig. 6 (A). The higher  $\text{Fr}$  yields a larger hydraulic gradient at an intersection.

The influence of ( $\beta$ ) as seen in Fig. 5 panel [4] affects the determination of the initial point of the hydraulic gradient at an intersection. Higher  $\beta$  produces larger  $\Delta L$  (see the description of  $\Delta L$  in Fig. 5 panel [1]). In this context, we drew a correlation between  $\beta$  with the non-dimensional parameter  $\Delta L/l_2$ . The last term indicates the ratio between initial points of the hydraulic gradient from the rearmost cell of a road prior to the intersection ( $\Delta L$ ) with the  $l_2$ . The result is presented in Fig. 6 (B), where ‘A’ denotes the amplitude of modeled waves. The result indicates that  $\Delta L$  will overlap  $l_2$  if  $\beta > 0.25$  because the flow depth starts to decline when the tsunami front has already passed the intersection. This means there will be no hydraulic gradient observed at the intersection even if the expansion ratio meets the criteria as explained previously. Therefore, in this condition, the maximum tsunami flow depth used for the design height will be the same for all sides of the intersection.

The above discussed phenomena were only observed in a flat topography scenario. We did not obtain similar results from sloping topography (1/100 and 1/50). Thus, dynamic features of tsunami flow at an intersection can only be used for consideration on determining the design height if the surrounding topography is relatively flat.

## 4. Conclusions

We evaluated the performance of pedestrian bridges by developing their fragility curves subjected to a tsunami from two perspectives. The first is the exposure in terms of their location from the shore; the second is the hazard characteristics in terms of the tsunami flow depths surrounding them. The results indicate that pedestrian bridges positioned in an area up to 1.2 km from the shore, or in an area where the estimated tsunami flow depths are 1.5 times that of

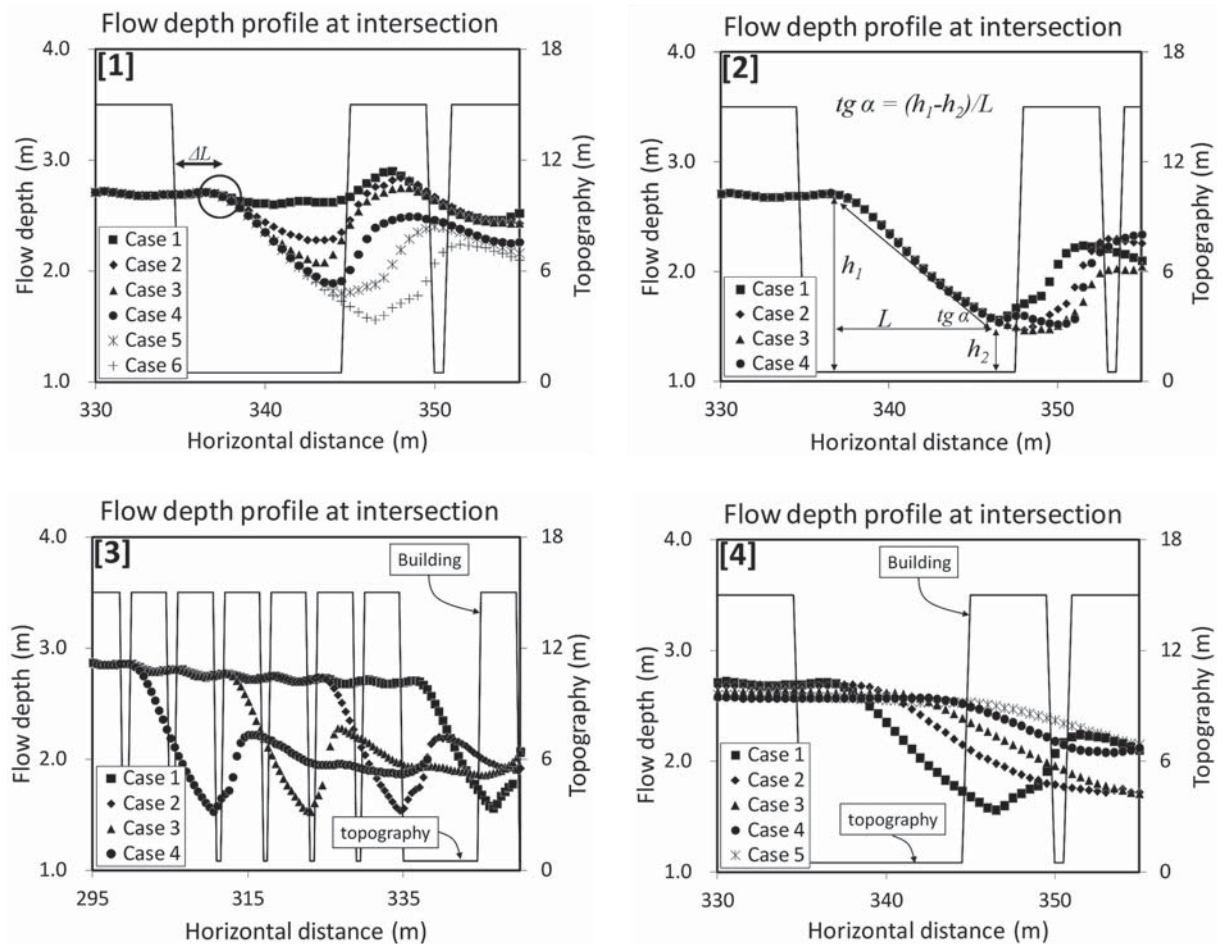


**Figure 5.** The influence of the following parameters to the modeled water surface at intersection (refer to panel [1] to [4]): [1] expansion ratio ( $D$ ), [2] road width parallel to the coastline ( $l_2$ ), [3] the length of residential block ( $l_1$ ) and [4]  $\beta$  (ratio between  $d_1$  and  $d_2$ )

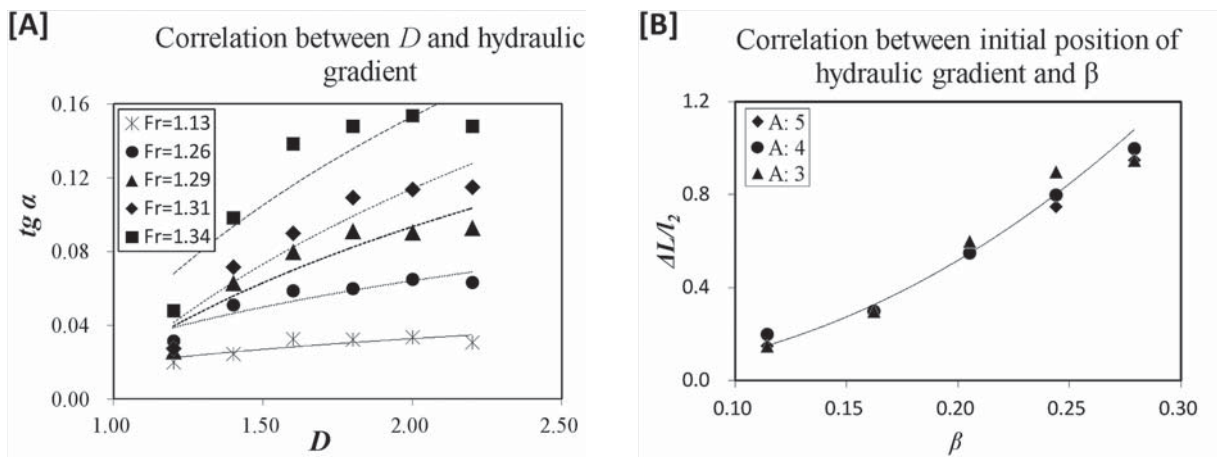


**Figure 6.** Plotting correlation between: [A] expansion ratio ( $D$ ) and hydraulic gradient ( $tg \alpha$ ), [B] correlation between the initial position of hydraulic gradient with the  $\beta$

the deck's height have a high probability of being damaged by a tsunami.

We discussed the opportunity of utilizing pedestrian bridges for evacuation in the areas described above by explaining the placement criteria based on tsunami flow characteristics at an intersection. The criteria were revealed by considering the dynamic features of tsunami flows at an intersection in a flat topographic condition. Depending on the estimated Froude number, intersections with geometric configuration that have an expansion ratio  $D > 1.5$  and  $\beta < 0.15$  may be appropriate for pedestrian bridges as vertical evacuation sites if they are installed on the landward side or on sides parallel to the coastline of an intersection.

### Acknowledgement

We are very grateful to the JST-JICA project (Multidisciplinary hazard reduction from earthquakes and volcanoes in Indonesia) group 3, and the Ministry of Education, Culture, Sports, Science and Technology (MEXT) Japan for financial support throughout study No.(22241042).

### References

- Cabinet Office, Internal Affairs and Communication Ministry, Fire and Disaster Management Agency and Meteorological Agency, 2011, Post-tsunami questionnaire survey, available at <http://www.yomiuri.co.jp/dy/national/T110817006318.htm>, last access March 2012.
- Fujima, F. (2012). Numerical simulation of the 2011 Tohoku tsunami in Miyako Bay, abstract for the Asian Oceania Geosciences Society (AOGS), Singapore, August 2012.
- Geospatial Information Authority of Japan (GSI), 2011, Information on Tohoku earthquake, available at [http://www.gsi.go.jp/BOUSAI/h23\\_tohoku.html](http://www.gsi.go.jp/BOUSAI/h23_tohoku.html), last access March 2012.
- Goto, C. and Shuto, N., 1983, Effect of large obstacle on tsunami inundation, *Tsunamis—Their science and engineering*, edited by: Iida, K. and Iwasaki, T., Terra Scientific Publishing Company, Tokyo, 511–525.
- Iemura H. and Pradono, M. H., 2006, Bridge damage survey in Banda Aceh and surrounding areas and earthquake and tsunami questionnaire. Proc. 4<sup>th</sup> International Conference on Earthquake Engineering, Taipei, Taiwan.
- Japan Society of Civil Engineers (JSCE), 2011, Tohoku earthquake-tsunami information, available at <http://www.coastal.jp/tsunami2011/>, last access March 2012.
- Karim, R. K. and Yamazaki, F., 2003, A simplified method of constructing fragility curves for highway bridges, *Earthquake Engineering and Structural Dynamic*, 32, 1603-1626.
- Koshimura, S., Oie, T., Yanagisawa, H., Imamura, F., 2009, Developing fragility function for tsunami damage estimation using numerical model and post-tsunami data from Banda Aceh, Indonesia, *Coastal Engineering Journal*, 51 (3), 243-273.
- Ministry of Land, Infrastructure and Transport (MLIT), 2011, Post-tsunami survey, available at <http://www.yomiuri.co.jp/dy/national/T110807002350.htm>, last access March 2012.
- Mori, N., Takahashi, T., Yasuda, T., Yanagisawa, H., 2011, Survey of 2011 Tohoku earthquake tsunami inundation and run-up, *Geophysical Research Letter*, 38, L00G14, doi:10.1029/2011GL049210.
- Muhari, A., Imamura, F., Koshimura, S., Post, J., 2011, Examination of three practical run-up models for assessing tsunami impact on highly populated areas, *Natural Hazard and Earth System Science*, 11, 3107-3123.
- Network for Earthquake Engineering Simulation (NEES), 2010, Development of Performance based Tsunami Engineering, PBTE, available at <https://nees.org/warehouse/project/664>, last access March 2012.
- Google, (2012), <https://maps.google.com/>, last access March 2012.
- Oliviera, P. J. and Pinho, F. T., 1997, Pressure drop coefficient of laminar Newtonian flow in axisymmetric sudden expansion, *Int. Journal of Heat and Fluid Flow*, 18, 518-529.
- Shinozuka, M., Feng, M. Q., Lee, J., Naganuma, T., 2000, Statistical analysis of fragility curves, *Journal of Engineering Mechanics*, 126 (12), 1224-1231.
- Shoji, G and Moriyama, T, 2007, Evaluation of the structural fragility of a bridge structure subjected to tsunami wave load, *Journal of Natural Disaster Sciences*, 29 (2), 73-81.
- Shuto, N., 1993. *Tsunami Intensity and Disasters, Tsunamis in the World*, 197-216.
- Southworth, F., 1991, Regional evacuation modeling: a state-of-the-art review. Oak Ridge National Labs, ORNL/TM-11740.